Accepted Manuscript

Submission Date: 2024-02-20
Accepted Date: 2024-04-29
Accepted Manuscript online: 2024-05-28

Seminars in Liver Disease

This is what MASLD looks like: Potential of a multiparametric MRI protocol

Anja M Fischer, Nazim Lechea, Harvey O Coxson.

Affiliations below.

DOI: 10.1055/a-2334-8525

Please cite this article as: Fischer A M, Lechea N, Coxson H O. This is what MASLD looks like: Potential of a multiparametric MRI protocol. Seminars in Liver Disease 2024. doi: 10.1055/a-2334-8525

Conflict of Interest: AMF, NL and HOC are employees of Boehringer Ingelheim Pharma GmbH & Co. KG.

Abstract:
Metabolic dysfunction associated steatotic liver disease (MASLD) is a prevalent condition with a broad spectrum defined by liver biopsy. This gold standard method evaluates three features: steatosis, activity (ballooning and lobular inflammation) and fibrosis, attributing them to certain grades or stages using a semi-quantitative scoring system. However, liver biopsy is subject to numerous restrictions, creating an unmet need for a reliable and reproducible method for MASLD assessment, grading and staging. Non-invasive imaging modalities, such as magnetic resonance imaging (MRI), offer the potential to assess quantitative liver parameters. This review aims to provide an overview of the available MRI techniques for the three criteria evaluated individually by liver histology. Here, we discuss the possibility of combining multiple MRI parameters to replace liver biopsy with a holistic, multiparametric MRI protocol. In conclusion, the development and implementation of such an approach could significantly improve the diagnosis and management of MASLD, reducing the need for invasive procedures and paving the way for more personalized treatment strategies.

Corresponding Author:
Dr. Anja M Fischer, Boehringer Ingelheim Pharma GmbH und Co KG, Clinical In Vivo Biomarkers, Birkendorfer Straße 65, 88400 Biberach, Germany, anja_2.fischer@boehringer-ingelheim.com

Affiliations:
Anja M Fischer, Boehringer Ingelheim Pharma GmbH und Co KG, Clinical In Vivo Biomarkers, Biberach, Germany
Nazim Lechea, Boehringer Ingelheim Pharma GmbH und Co KG, Clinical In Vivo Biomarkers, Biberach, Germany
Harvey O Coxson, Boehringer Ingelheim Pharma GmbH und Co KG, Clinical In Vivo Biomarkers, Biberach, Germany

This article is protected by copyright. All rights reserved.

Accepted Manuscript

This is a PDF file of an unedited manuscript that has been accepted for publication. As a service to our customers we are providing this early version of the manuscript. The manuscript will undergo copyediting, typesetting, and review of the resulting proof before it is published in its final form. Please note that during the production process errors may be discovered which could affect the content, and all legal disclaimers that apply to the journal pertain.

Thieme

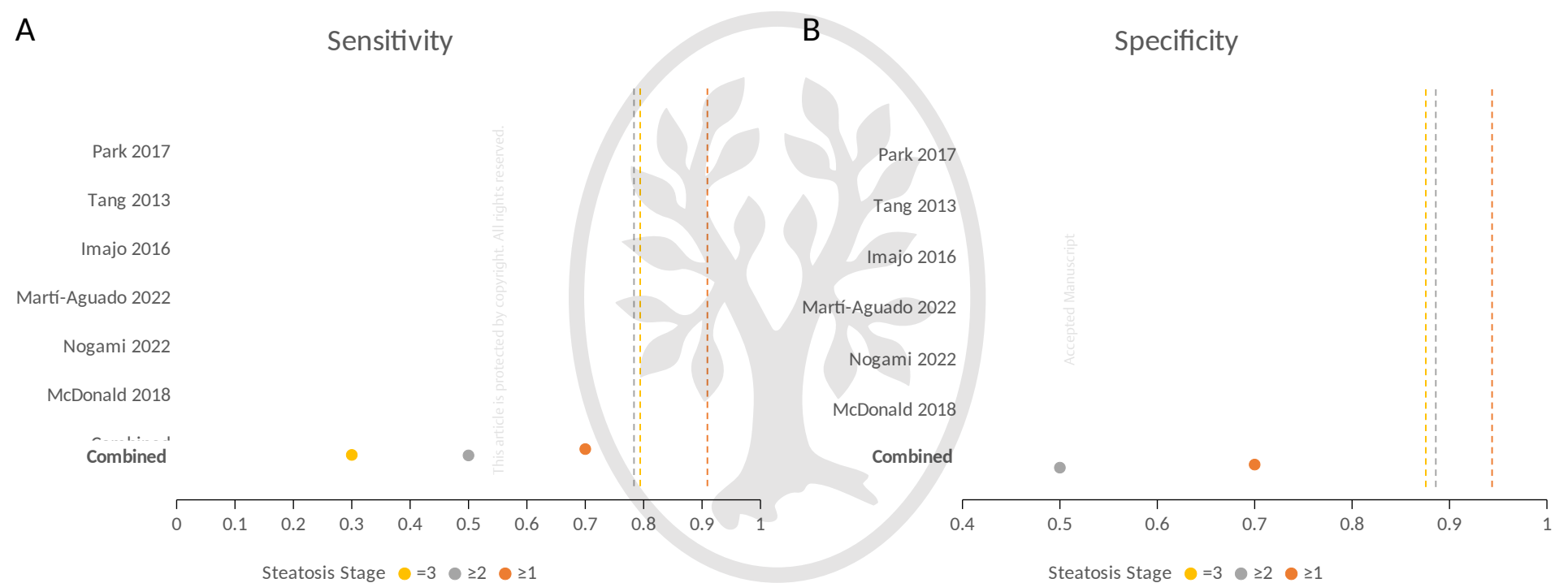

This article is protected by copyright. All rights reserved.
Accepted Manuscript

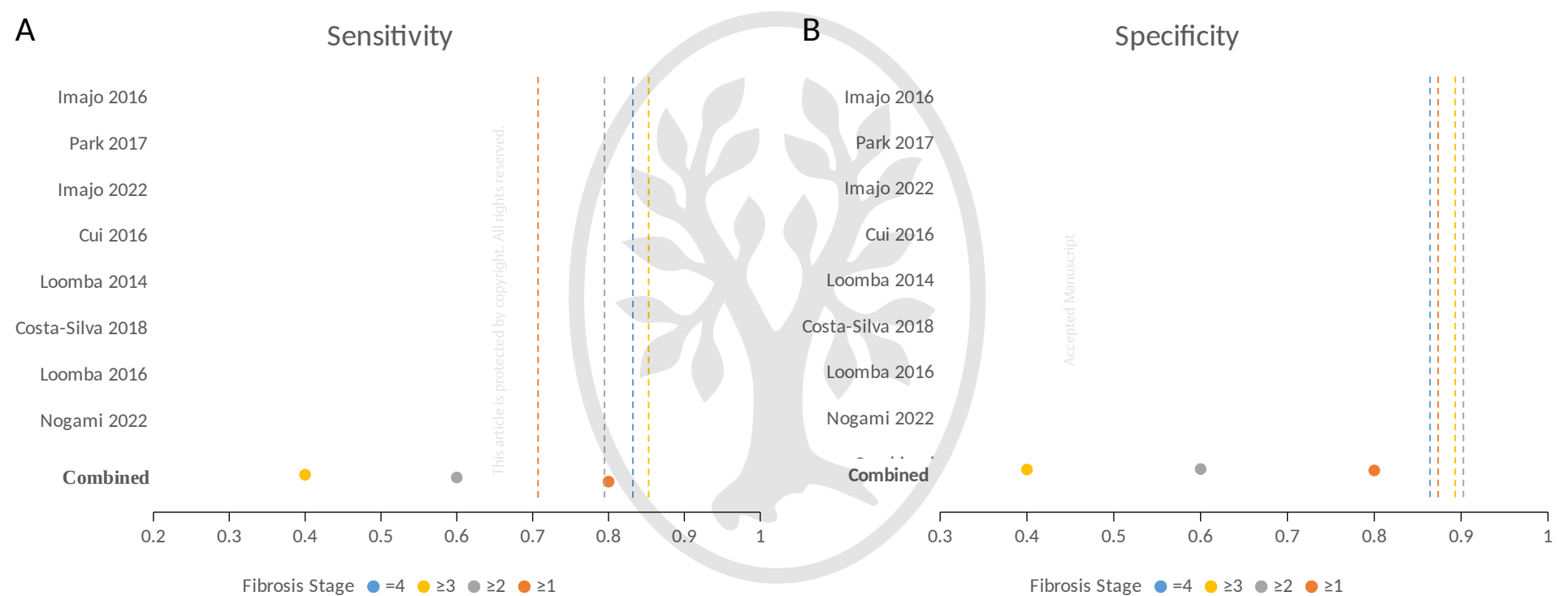

This article is protected by copyright. All rights reserved.
Accepted Manuscript

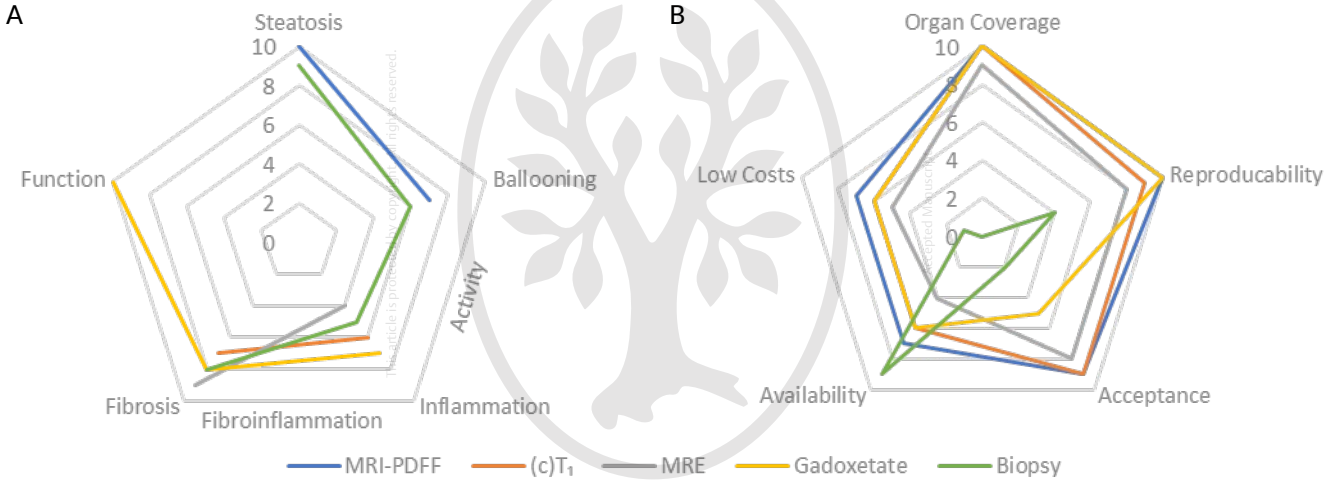

This article is protected by copyright. All rights reserved.
Accepted Manuscript

This is what MASLD looks like: Potential of a multiparametric MRI protocol

Anja M Fischer, PhD[1], Nazim Lechea, PhD[1], Harvey O Coxson, PhD[1]

[1]Boehringer Ingelheim Pharma GmbH & Co. KG, Biberach, Germany

Corresponding Author:

Mrs. Anja Maria Fischer, PhD

anja_2.fischer@boehringer-ingelheim.com

This article is protected by copyright. All rights reserved.

Accepted Manuscript

Abstract

Metabolic dysfunction associated steatotic liver disease (MASLD) is a prevalent condition with a broad spectrum defined by liver biopsy. This gold standard method evaluates three features: steatosis, activity (ballooning and lobular inflammation) and fibrosis, attributing them to certain grades or stages using a semi-quantitative scoring system. However, liver biopsy is subject to numerous restrictions, creating an unmet need for a reliable and reproducible method for MASLD assessment, grading and staging. Non-invasive imaging modalities, such as magnetic resonance imaging (MRI), offer the potential to assess quantitative liver parameters. This review aims to provide an overview of the available MRI techniques for the three criteria evaluated individually by liver histology. Here, we discuss the possibility of combining multiple MRI parameters to replace liver biopsy with a holistic, multiparametric MRI protocol. In conclusion, the development and implementation of such an approach could significantly improve the diagnosis and management of MASLD, reducing the need for invasive procedures and paving the way for more personalized treatment strategies.

Key words: metabolic dysfunction associated steatotic liver disease, magnetic resonance imaging, non-invasive tests, liver stiffness, hepatocyte function

Lay Summary

- A multi-parametric MRI protocol estimating liver fat content, extracellular water, liver stiffness and hepatocyte function captures a whole organ holistic picture of the liver structure and function.
- Different MRI methods assess different features of MASLD and not every question necessitates the complete range of MRI techniques.
- The most valuable MRI method largely depends on the specific stage within the MASLD spectrum or question that is being investigated.

Introduction

The rise of metabolic dysfunction associated steatotic liver disease (MASLD) globally demands urgent attention and innovative diagnostic approaches to combat its progression and devastating consequences[1]. This surge in MASLD, and its more severe form, metabolic dysfunction associated steatohepatitis (MASH), is closely linked to the escalating rates of obesity, type 2 diabetes, and metabolic syndrome, further complicated by genetic factors[2–7]. Moreover, the progressive fibrosis in advanced MASH can lead to cirrhosis and the development of other severe outcomes including hepatocellular carcinoma and portal hypertension[8,9]. To effectively address this growing health concern, it is crucial to gain a comprehensive understanding of the pathogenesis of MASLD and MASH, as this knowledge will pave the way for the development of novel and targeted treatments. Clinical imaging plays a vital role in elucidating the underlying mechanisms of this disease, enabling researchers and clinicians to identify potential therapeutic targets and monitor treatment efficacy. By focusing on the intricate interplay between disease pathogenesis and innovative diagnostic

This article is protected by copyright. All rights reserved.

Accepted Manuscript

techniques, the medical community can work towards more effective strategies to manage and ultimately conquer these prevalent and potentially life-threatening liver diseases.

While the disease processes of MASLD/MASH have many systemic manifestations, the ultimate diagnosis relies on a histologic description of a biopsy sample. This assessment is commonly performed using three main semi-quantitative scores: steatosis, activity (ballooning and lobular inflammation), and fibrosis[10,11]. Although considered the "gold standard", this approach has limitations due to the invasiveness of the procedure, small specimen volume (approximately 1/50,000 of the liver[12]), and the semi-quantitative nature of the assessment[13]. These factors contribute to the low agreement rate of paired biopsy samples and complicate diagnosis and the determination of endpoints in late-stage MASH-related clinical trials[14–16].

To address these challenges, the United States Food and Drug Administration (FDA) recommends integrating and evaluating non-invasive biomarkers, including clinical imaging biomarkers[17,18]. Magnetic resonance imaging (MRI) is emerging as a popular choice among imaging techniques due to its versatility and accuracy. However, while histology assesses multiple pathologic features of MASLD (steatosis, activity, and fibrosis), non-invasive imaging techniques are typically limited to assessing one feature at a time. Thus, it is crucial to match the appropriate imaging method with the specific question and location within the MASLD spectrum.

This review aims to provide an overview of available MRI techniques relating to the three histologic features of MASLD, as described above and summarized in Table 1. MRI offers a diverse array of methodologies, from widely accepted MRI fat quantification (proton density fat fraction (PDFF)) and measurement of the longitudinal relaxation time (T_1) to more exploratory approaches like gadoxetate-based methods. While these acquisition techniques are preinstalled on most clinical scanners the MRI portfolio is complemented by commercial MRI products, including hardware devices and software imaging analysis methods. For example, magnetic resonance elastography (MRE), which enables the assessment of mechanical tissue parameters and requires secondary

This article is protected by copyright. All rights reserved.
Accepted Manuscript

hardware and the proprietary iron-corrected T_1 (cT_1) method which corrects iron-induced bias and standardizes across scanners and field strengths. In this article, we will discuss these techniques and their applications in greater detail for each disease manifestation. Lastly, we will emphasize the importance of combining multiple methods to capture a comprehensive picture of MASLD and propose a multiparametric MRI acquisition protocol.

Assessment of steatosis

The primary characteristic and defining feature of MASLD is the accumulation of triglycerides as fat droplets within hepatocytes. These fatty acids originate from various sources, including serum non-esterified fatty acids (59%), de novo lipogenesis (26%), and dietary fatty acids (15%)[19,20]. Fat droplets can be classified as either microvesicular or macrovesicular steatosis based on their size. In MASLD, macrovesicular steatosis is the predominant pattern, characterized by medium to large fat droplets and the displacement of the hepatocyte nucleus to the periphery[11,19,21]. To diagnose MASLD, at least 5% of hepatocytes must exhibit fatty acid accumulation in the form of macrovesicular steatosis[21].

MRI-PDFF

The signal accessible using conventional ^{1}H MRI almost exclusively originates from the hydrogen nuclei of either triglycerides or water and the chemical structure of these molecules is characterized by distinct magnetic resonance (MR) frequencies. It was recognized early on that magnetic resonance spectroscopy (MRS) could quantify the proportion of fat molecules relative to the sum of water and fat molecules. However, while MRS shows excellent accuracy and sensitivity for the assessment of fat content and allows for further characterization of the lipids it is a complicated procedure with limited coverage and is not available in all clinical centers. Hence, researchers devised sophisticated techniques such as multi-echo Dixon methods and advanced fat water separation algorithms, specifically the Iterative Decomposition of water and fat with Echo Asymmetry and Least-squares estimation (IDEAL). These methods have proven effective in achieving robust fat-water separation, eliminating the T_1 or T_2* bias that can affect quantification. This IDEAL-

This article is protected by copyright. All rights reserved.
Accepted Manuscript

PDFF technique shows excellent performance compared to MRS across magnetic field strengths, MRI manufacturers and reconstruction methods[22] and a high level of concordance with liver biopsy in multiple studies[18,23–27]. A meta-analysis of the published data reveals the greatest combined sensitivity (0.92) and specificity (0.95) of MRI-PDFF in distinguishing steatosis at stage 1 or above, determined histologically, from no steatosis. The reduced sensitivity in detecting more advanced stages aligns with a recent study examining the discrepancy between MRI-PDFF and histology[28]. Here discrepancy was reported to be primarily due to MRI-PDFF underestimating the advanced stages reported by histology. Forest plots on sensitivity and specificity are summarized in Figure 1 for all steatosis stages. In addition to the overall high performance of MRI-PDFF, Noureddin et al. reported a higher sensitivity to small, longitudinal changes in hepatic fat compared to liver biopsy[29]. These findings were attributed to the low reproducibility and the broad grading categories associated with liver biopsy[29] while a study on the repeatability of MRI-PDFF proposed a threshold of 1.2 to 1.6% to discern real change from measurement error[30]. Furthermore, the inter-reader agreement of MRI-PDFF (ICC = 0.998-0.996)[31] outperforms liver biopsy (ICC = 0.654)[32] and ultrasonography-based methods for liver fat quantification. For these reasons, MRI-PDFF is widely accepted and even recommended for early clinical trials as primary efficacy endpoint especially in drugs suspected to have an anti-steatotic effect[33]. FDA- and European Medicines Agency (EMA)-approved MRI sequences with CE-marked on-scanner reconstruction of the PDFF maps are provided for different vendors (GE, Philips, Siemens and Canon) promoting MRI-PDFF as a widely available technique for precise and non-invasive hepatic steatosis assessment.

The main advantage of MRI-PDFF over both biopsy and MRS is the whole organ coverage and the additional possibility for spatial assessment, enabling evaluation of heterogeneity within and between liver segments. The heterogeneity in this context necessitates a reliable and consistent segmentation process for extracting features. To address this, recent investigations focus on automated liver segmentation and processing of median PDFF[25].

This article is protected by copyright. All rights reserved.

Accepted Manuscript

In addition to the spatial distribution, characterization of the spectral information might allow future advantages such as triglyceride differentiation. Due to its complex chemical structure (hydrogen atoms are residing at different sites in the molecule), the MR signal of triglycerides contains multiple MR frequencies, and the spectral frequency pattern can possibly be used to quantify the underlying fatty acid composition. Current techniques (i.e., IDEAL) predefine the fatty acid composition and ignore potential deviations but different approaches are currently under investigation which provide additional information on the share of saturated, mono- and polyunsaturated fatty acids[34–36]. Since recent studies suggest an interdependence of the fatty acid composition and the severity of MASLD, linking severe phenotypes to an increased share of saturated fatty acids, the characterization of the triglyceride signal pattern might allow for patient segmentation or stratification[37].

In conclusion, MRI-PDFF is a widely available and accepted method for the quantification of liver fat that still has the potential to generate additional characterization and benefit in the near future by application of new yet experimental postprocessing techniques.

Assessment of activity

Simple steatosis is the most common form of MASLD, and the majority of patients remain at this low end of the broad MASLD spectrum for several years. However, it has been reported that approximately one third progresses to the more severe form of MASH[2,5,38]. In MASH, hepatocyte activity is disrupted due to the presence of inflammation, and liver cell damage (hepatocyte ballooning). These factors can lead to impaired liver function and, in severe cases, progress to liver fibrosis, cirrhosis, or liver cancer[20,21]. The inflammation and ballooning features are separately assessed by histology and are often collectively referred to as activity[10,11,21].

Currently, the most challenging aspect of MASLD to evaluate using MRI is assessing activity[39]. At present, no specific approach is designed for differentiating activity grades; instead, existing techniques for steatosis and fibrosis assessment are extended to encompass this aspect of the disease. This is partly due to the simultaneous development and progression of various pathological

This article is protected by copyright. All rights reserved.
Accepted Manuscript

features in hepatic tissue. Additionally, ballooning and inflammation have distinct effects on different MRI methods, making a combination of multiple techniques potentially the most promising approach for assessing activity.

MRI-PDFF to assess ballooning

Ballooning is the histologic term for swelling and rounding of the hepatocyte due to a manifestation of cell injury and altered accumulation of fat droplets[40]. Since MRI-PDFF is a measure of liver fat content, investigators have tried, with varying degrees of success, to link MRI-PDFF to ballooning grade. Although, studies investigating the interplay of ballooning and MRI markers are sparse, some report a correlation of PDFF and histologic ballooning grade and changes thereof[41–43] while others do not find a correlation[44]. However, it must be emphasized that the status of liver biopsy as a reference is particularly questionable for this MASLD feature since inter-reader agreement is very low (ICC = 0.012)[32] and only moderate agreement can be obtained between paired liver biopsy samples[14].

MRE to assess inflammation

Elastography is the objective and quantitative evolution of palpation, which for many decades was the only opportunity to assess mechanical properties of abdominal organs. Nowadays, different imaging technologies quantitatively capture these features by accessing the propagation characteristics of shear waves in tissues. The most objective and reproducible amongst these techniques is MRE. Briefly, this approach uses a commercially available external driver to generate vibrations at 60Hz and acquires complex MR raw data under application of an additional motion encoding gradient[45]. Since the speed of shear waves differs significantly across different types of soft tissues, this variation is used to distinguish between tissues and to assess pathophysiological changes[46]. The behavior of the shear waves is determined by the shear modulus which refers to the deformability of the tissue in response to shear stress. The magnitude of the shear modulus (shear stiffness) is the quantity most frequently assessed by MRE and is often also designated as stiffness. However, it represents the combined effect of two distinct material properties: elasticity and

This article is protected by copyright. All rights reserved.
Accepted Manuscript

viscosity[46]. The former is attributable to the characteristics of solids and refers to a reversible deformation resulting in a storage of energy (storage modulus) while the latter is associated with the behavior of fluids and represents an irreversible deformation and dissipation of energy (loss modulus). Hepatic inflammation is associated with the accumulation of free fluids in the inter-hepatic space, which would, in theory, result in an alteration of shear stiffness due to a changed loss modulus (viscosity). While there is therefore great interest in the application of MRE for the assessment of inflammation, the shear stiffness in the liver is largely determined by the elasticity related storage modulus component. Thus, changes in the shear modulus are strongly dominated by fibrotic processes. Hence, it is not surprising that while some studies demonstrate a correlation between inflammation status and shear modulus[47–49] other studies do not[50]. In this context hope is placed on the development of new 3D MRE techniques which allow the separate assessment of the viscous tissue characteristics. For example, while there is limited data in the MASH population, a recent 3D MRE study of hepatitis B and C patients retrieved AUROCs of 0.86-0.90 for different stages of inflammation[51]. However, it must be noted that at this point 3D MRE is still an experimental technique.

MRI-PDFF and MRE – Yin and Yang of activity assessment?

Leveraging the described correlation of MRI-PDFF and hepatic ballooning, as well as inflammation and MRE, various studies have been conducted in both mice[48] and humans[47,52,53] combining these two techniques. This approach demonstrated increased performance in diagnosing MASH and assessing activity scores. The enhanced effectiveness can be attributed to the sensitivity of MRI-PDFF to hepatic ballooning and of MRE to lobular inflammation, which together define histology-based activity[52]. Consequently, MRI-PDFF and MRE can be viewed as two contrasting techniques that, when used in tandem, provide a holistic picture of hepatic activity.

This article is protected by copyright. All rights reserved.

Accepted Manuscript

(c)T_1 and Gadoxetate – Alternatives to MRE for inflammation assessment?

Fluid in the inter-hepatic space impacts the relaxation behavior of the MR signal. In particular, T_1 increases with fluid content and has been associated with inflamed hepatic tissue. However, multiple other factors such as fibrosis, fat fraction, hydration, iron content, glucose, ascites and edema impact this relaxation constant. Thus, the ambiguity of the results obtained by T_1 relaxometry in relation to inflammation grade assessed by histology is not surprising: while most studies report a positive correlation of T_1 and inflammation grade[43,50,54,55], some conclude no relation[56], and one study in rats found a negative correlation[57].

For these reasons, investigators have tried to quantify extracellular volume using contrast-enhanced MRI. In hepatic MRI two classes of contrast agents are applied: extracellular and hepatobiliary contrast agents which differ regarding their pharmacokinetics[58]. While both initially accumulate in the extracellular space, hepatobiliary contrast agents (i.e., gadoxetate disodium) are subsequently in part actively taken up by healthy hepatocytes and excreted via the biliary system (the dual function of these contrast agents is described in more detail in the section on fibrosis). Based on a dynamic acquisition and a multi-compartment model, insights on extracellular volume can be derived from gadoxetate-enhanced MRI[59]. However, this approach requires advanced mathematical models and is still experimental. There is interesting data that suggests an impact of steatohepatitis on the liver-kinetics underlying hepatobiliary contrast agents[60,61], but currently, there is a lack of information regarding the performance of this technique correlating extracellular volume and inflammation.

Assessment of fibrosis

Inflammation is a necessary component of healing processes[62]. However, in 20% of MASH patients protracted wound healing of liver tissue eventually culminates in liver fibrosis[20,63–65]. This accumulation of extracellular matrix proteins is the direct result of an imbalance of fibrogenesis and fibrolysis due to an uncompensated shift towards a reparative, anti-inflammatory immune response which is initiated by signaling from damaged or stressed hepatocytes and activated

This article is protected by copyright. All rights reserved.
Accepted Manuscript

macrophages[20,63,66]. Given the close link of inflammation and fibrosis it is not surprising that they are driven by comparable factors such as genetic predisposition and interaction with intestine and adipose tissue[3,63,67–69]. However, the severity of fibrosis rather than the degree of steatosis or activity predicts liver-related and overall morbidity and mortality in MASLD patients[38,70]. For this reason, fibrosis is staged independently of activity based on location and amount of extracellular matrix proteins[10,11] and non-invasive fibrosis biomarkers are also of interest for the prediction of liver-related outcomes. In summary, fibrosis describes the remodeling of hepatic tissue by extracellular matrix proteins – mainly type I/III collagen[71].

MRE

The increasingly organized structure of the collagen fibers results in a reduction of the elasticity of the liver which dominates the storage modulus assessed by MRE. For this reason, MRE is considered the most promising MR-technique to assess liver fibrosis. Standard clinical MRE generates 2D elastograms representing the magnitude of the shear modulus which is used to calculate liver stiffness. Multiple studies applied this standardized approach to evaluate its performance to differentiate biopsy accessed fibrosis stages[18,23,27,72–76]. A meta-analyses based on the pooled data of these studies revealed the best performance for the detection of a fibrosis stage of 3 or above with a combined sensitivity of 0.86 and specificity of 0.90. The detection of at least fibrosis stage 1 yielded the lowest summary sensitivity (0.71) and a specificity of 0.88. A detailed overview of the results of the meta-analysis is provided in Figure 2. Overall, the AUROC of MRE increases with advancing fibrosis and is reported to outperform ultrasonography-based techniques in advanced stages[72]. Furthermore, inter-reader agreement of MRE (ICC = 0.948[72] & ICC = 0.84[77]) is higher than those acquired for vibration controlled transient elastography (ICC = 0.790)[72] and biopsy (ICC = 0.504)[32]. It is suggested that a threshold of 0.75 kPa represents a significant change in MRE[30]. The main limitations of MRE, aside from the limited availability of the MRE hardware, are the sensitivity of MRE to early stages of fibrosis and a reduced reliability in the presence of iron. Specifically, the elastograms are provided with an area of confidence representing a region of sufficient signal

This article is protected by copyright. All rights reserved.
Accepted Manuscript

intensity. In cases of iron overload, particularly at 3T, this area might shrink. In rare occasions, this could culminate in technical failure[78]. Therefore, alternative techniques such as the usage of spin-echo based echo planar imaging sequences especially at 3T to reduce the impact of iron[79] and 3D MRE, which allows for the extraction of additional variables (discussed in more detail in the previous section on activity) are increasingly being applied with novel automated analysis techniques to improve the sensitivity of MRE in all conditions.

(c)T_1

The most prominent alternative to MRE is the measurement of the longitudinal relaxation time T_1. As previously mentioned, T_1 is a multi-dependent MR signal property and initially gained attention in cardiac MRI. Common applications of MRI involved acquiring images using T_1-weighted contrast sequences which display grey scale values that are closely related to the T_1 relaxation time. However, these techniques are less sensitive to small changes in T_1, particularly in cardiac MRI, and do not allow the proper assessment of fibrosis. While the extraction of actual T_1 values was thought to be valuable, this technique required multiple breath-holds which limited applicability in cardiac MRI. This limitation led to the development of new acquisition sequences and post-processing algorithms that enabled the acquisition of T_1 maps in a single breath-hold displaying the actual T_1 values, measured in milliseconds[80]. This significant advancement catalyzed the application of T_1 quantification in other organ systems such as the liver. However, it is worth noting that T_1 also depends on both tissue characteristics such as the presence of edema, fatty acids and iron as well as scanner characteristics like the field strength. Therefore, caution is required when interpreting T_1 maps, especially in organs such as the liver where confounding features are frequently present. For these reasons it is not surprising that fibrosis staging by T_1 was outperformed by MRE despite a high inter-reader agreement of ICC = 0.94-0.993[50,77].

Recently, post-processing algorithms have been developed to minimize the impact of the competing influences on T_1. The technique to correct for the effect of iron load in the liver is based on the transverse relaxation time (T_2*) and is referred to as iron-corrected T_1 (cT_1)[81]. This correction was

This article is protected by copyright. All rights reserved.
Accepted Manuscript

further extended to standardize to a specific scanner from a specific vendor at a specific field strength to obtain a reproducible, scanner-independent MRI marker to assess extracellular water content[81,82]. This approach has been commercialized and is available through the patent holder.

Multiple studies have reported an increase in cT_1 with fibrosis stage, particularly in the early stages of the fibrotic process[56,83,84]. However, due to the effect of inflammation on T_1, which also raises cT_1 values[84], this measure is collectively referred to as fibro-inflammation. Additionally, steatosis grade is positively associated with cT_1 and is the strongest among multiple confounding factors in MASLD[79,81,82]. Since steatosis is the key feature of MASLD across the disease spectrum and often decreases in advanced stages of fibrosis, the confounding of cT_1 by changes in fat content is a significant concern. Consequently, it becomes challenging to determine whether a decrease in cT_1 is primarily caused by fibrosis, inflammation, or steatosis regression.

While T_1 quantification is available on most MR scanners, the availability of cT_1 is restricted since it requires an additional commercial product and might be inconclusive for high iron overload (>5mg Fe/g dry tissue) and high fat content (>35%: no cT_1 reported)[85]. Importantly though, cT_1 and T_1 both cover the entire organ and should allow regional disease assessment.

Gadoxetate enhanced imaging

As previously mentioned in the section on inflammation, gadoxetate, also known as gadoxetic acid, is a liver-specific contrast agent used in MRI to enhance the visualization of liver lesions. Gadoxetate is partly taken up by hepatocytes through an active transport mechanism involving the organic anion transporting polypeptides (OATPs). Once inside the hepatocytes, gadoxetate is excreted into the bile canaliculi through the multidrug resistance-associated protein 2 (MRP2). Under normal condition 50% of the contrast agent follows the described hepatobiliary route while the other 50% are removed via the systemic circulation. The hepatobiliary route of the contrast agent allows for the enhancement of healthy liver parenchyma and enables the assessment of hepatocyte function as the gadoxetate is only transported into the biliary system by functional hepatocytes[58].

This article is protected by copyright. All rights reserved.
Accepted Manuscript

The bifunctional pharmacokinetic pattern of gadoxetate allows for the extraction of different contrasts depending on the delay after contrast injection. The assessment of the contrast agent within the intra- and extracellular space is accomplished by measuring the MR signal throughout the late arterial (30-35s after contrast injection) and portal phase (60-75s). The active transport by hepatocytes starts in the translational phase (3-5min) and reaches maximum parenchymal enhancement during the hepatobiliary phase (15-20min)[58]. This pharmacokinetic pattern allows for both static and dynamic approaches to derive measures of hepatocyte health. Static techniques are usually performed with high spatial resolution at a single time point during hepatobiliary phase and are evaluated either for a region of interest or the whole liver. The most common static technique compares MR signal intensity (T_1-weighted) obtained in the hepatobiliary phase (usually 20min after injection) to pre-contrast values. This relative liver enhancement yielded the highest inter-reader repeatability (ICC = 0.979)[86] among all static techniques and has an AUROC of 0.93 to 0.98 for the differentiation of histologically determined fibrosis stages[87]. Moreover, in a study in 98 participants, these data showed a decrease in signal intensity in advanced liver fibrosis[87]. Other static techniques use reference tissues as muscle or spleen, or calculate T_1 relaxation time to provide a less scanner dependent measure[61].

The potential advantage of gadoxetate imaging is to move beyond static techniques and examine the dynamic uptake of gadoxetate by functional hepatocytes. Instead of acquiring a single image during hepatobiliary phase and comparing it to pre-contrast, a continuous acquisition of images is performed starting from the contrast injection and continuing until the hepatobiliary phase. This extended acquisition process lasts approximately 20 minutes for individuals with normal liver function. However, in advanced stages or when there is a need to capture additional variables related to biliary excretion, an extension of the acquisition duration might be necessary[88]. A complete data set allows quantitative measures of hepatocyte transport and perfusion to be derived using multi-compartment analysis or deconvolution models[61]. Unfortunately, due to the demanding mathematical models for extraction of the desired variables studies applying dynamic techniques are

This article is protected by copyright. All rights reserved.
Accepted Manuscript

sparse and mostly restricted to animal models[89,90], although a study in chronic hepatitis patients yielded an AUROC of 0.701 for the differentiation of no versus mild fibrosis[91].

While gadoxetate is an accepted contrast agent in detection and characterization of focal liver lesions, its application in staging liver fibrosis is currently considered investigational[92]. However, the increasing prevalence of MASLD combined with the possibility of simultaneous screening for hepatocellular carcinomas, the prevalence of which is increased in MASLD[8], and the promising results of recent studies might set the stage for a broader field of clinical application.

Multiparametric MRI protocol/Challenges and Limitations

MRI techniques are powerful multifaceted techniques that allow the assessment of histologic features of MASLD/MASH. Studies have shown that MRI captures a whole organ holistic picture of the liver structure and function. However, there is not one MRI technique that allows quantification of all the different features of MASLD/MASH. Therefore, multiple techniques may be needed to get the whole picture of the disease process. For example, a "suite" of MRI imaging that quantifies tissue composition (i.e., fat content by MRI-PDFF and extracellular water by (c)T_1) and tissue mechanical properties (MRE), will cover the grading of steatosis, activity and fibrosis usually only assessed using histology (Figure 3). Additionally, MRI allows for the assessment of hepatocyte function using gadoxetic acid. This yet experimental gadoxetate imaging approach captures a further color of the MASLD spectrum not accounted for by histology (Figure 4) since it allows for the quantification of both liver structure and function.

However, it is important to note that not every question necessitates the complete range of MRI techniques. The most valuable MRI method largely depends on the specific stage within the MASLD spectrum or question that is being investigated. For instance, in the early stages, MRI-PDFF for steatosis assessment and (c)T_1 for steatohepatitis detection may be adequate. These techniques can

This article is protected by copyright. All rights reserved.
Accepted Manuscript

also be utilized for screening MASLD or identifying at-risk MASH in large cohort studies[93]. Additionally, MRI-PDFF is used in early clinical trials to assess treatment response[94–96]. On the other hand, lower liver fat in individuals with advanced fibrosis or cirrhosis was associated with worse outcome[97]. Therefore, MRE and gadoxetic acid-enhanced MRI may be more advisable for more advanced stages. While gadoxetic acid-enhanced MRI is a yet experimental technique in the context of MASLD, MRE alone or in combination with other clinical indicators was reported by different studies to be a predictor of liver-related events[98–100]. In conclusion, it is important to fully understand the disease process within the MASLD spectrum, the expected histological changes and the reason for the imaging technique before applying it. Figure 5A is intended to assist in the selection of the appropriate MRI technique(s). The netplot provides an overview of the performance of the covered MRI techniques for different MASLD features in comparison to biopsy. It is important to keep in mind that even though biopsy-based histology is considered the "gold standard" it still shows limited performance due to sampling error, limited organ coverage and low reproducibility[32]. These criteria and the higher acceptance and quantitative nature represent the strongest advantages of a multiparametric MRI protocol over liver biopsy as is visualized in Figure 5B. Importantly, due to its non-invasiveness, multiparametric MRI is well suited to screening and follow-up settings in clinical trials.

However, as Figure 5B further indicates, MRI is also facing challenges. The most obvious and often quoted challenges are availability and cost, albeit the costs are still lower than those associated with liver biopsy[56,74,101,102]. Ultrasonography-based techniques are non-invasive alternatives that benefit from low costs and relatively broad availability[72]. While ultrasonography is a commonly applied approach within MASLD/MASH, these techniques do not achieve the accuracy and reproducibility of MRI[18,23,72,73]. Therefore, cost-effectiveness analyses predominantly rule in favor of MRI[103] and this should only become better as the availability of MRI increases in the future[101].

This article is protected by copyright. All rights reserved.

Accepted Manuscript

Concluding Remarks

It is important to keep in mind that the histologic evaluation of a liver biopsy limits investigators to a single snapshot in time of an extremely small sample of the liver. Moreover, biopsy is not an easy procedure and includes risk to the participant. MRI, on the other hand, allows full organ coverage, which strengthens the results in a complex disease such as MASLD. Furthermore, experts agree that there need to be validated and useful non-invasive tests for this disease. Recently there is a growing interest in composite biomarkers that combine imaging with non-imaging biomarkers. One example is the prediction of treatment response by a combination of MRI-PDFF with blood-based biomarkers[104,105]. Other composite markers which include MRE are mainly intended to predict outcome in more advanced stages. The most established amongst them is the MAST score which includes aspartate aminotransferase measured in blood with MRI-PDFF and MRE[106]. A second recent score is the MEFIB which combines MRE and FIB-4 score for MASH and advanced fibrosis detection[107]. Both composites were shown to be associated with liver related events while MEFIB was reported statistically superior in predicting hepatic decompensation[108]. Other studies confirm the performance of MEFIB for prediction of decompensation and death[98,99]. Additionally MRI opens the possibility of analyzing the spatial distribution of certain features throughout the organ. Nonetheless, examining the entire liver does not fully encompass the scope of the issue, as MASLD represents the hepatic manifestation of metabolic syndrome and is significantly impacted by other organs, such as various adipose tissue compartments or the intestine. Therefore, one benefit of MRI is the simultaneous accessibility of multiple organs. For example, PDFF-maps or T_1 images of the abdomen, allow the volumetric quantification of different abdominal adipose tissue compartments. Recent studies have shown that the prevalence of MASLD and MASH was found to increase with visceral adipose tissue volume, while no difference was observed for subcutaneous adipose tissue[109,110]. In addition, inflammation of visceral adipose tissue which might be revealed by T_1 increase is associated with hepatic fibro-inflammation[111].

This article is protected by copyright. All rights reserved.

Accepted Manuscript

Furthermore, a potential complication of hepatic cirrhosis is portal hypertension caused by increased intrahepatic resistance and representing a necessary condition for multiple MASLD associated comorbidities (i.e., esophageal varices and ascites)[112]. Recent studies suggest that the simultaneous assessment of spleen stiffness (shear or loss modulus) during 3D MRE examination of the liver is a reliable non-invasive indicator for portal hypertension[51,113]. Thus, the coverage of the spleen in addition to the liver by MRE might allow for risk stratification of certain comorbidities in advanced fibrosis.

In conclusion, a multiparametric MRI protocol not only covers the entire liver volume and MASLD spectrum with additional information on hepatocyte function but also allows for segmentation of disease based on related extrahepatic alterations. We argue that this is clearly better than the histological assessment of unviable liver fragments and can be applied across multiple centers in multiple studies and provides investigators with a method to assess disease pathogenesis and response to therapy.

Conflict of Interest

AMF, NL and HOC are employees of Boehringer Ingelheim Pharma GmbH & Co. KG.

1. Younossi, Z. M. *et al.* The global epidemiology of nonalcoholic fatty liver disease (NAFLD) and nonalcoholic steatohepatitis (NASH): a systematic review. *Hepatology* **77**, 1335–1347 (2023).

2. Moore, J. B. Non-alcoholic fatty liver disease: the hepatic consequence of obesity and the metabolic syndrome. *P Nutr Soc* **69**, 211–220 (2010).

3. Eslam, M. *et al.* MAFLD: A Consensus-Driven Proposed Nomenclature for Metabolic Associated Fatty Liver Disease. *Gastroenterology* **158**, 1999-2014.e1 (2020).

4. Younossi, Z. M. *et al.* Global epidemiology of nonalcoholic fatty liver disease—Meta-analytic assessment of prevalence, incidence, and outcomes. *Hepatology* **64**, 73–84 (2016).

5. Haas, J. T., Francque, S. & Staels, B. Pathophysiology and Mechanisms of Nonalcoholic Fatty Liver Disease. *Annu Rev Physiol* **78**, 1–25 (2015).

6. Cotter, T. G. & Rinella, M. Nonalcoholic Fatty Liver Disease 2020: The State of the Disease. *Gastroenterology* **158**, 1851–1864 (2020).

7. Radu, F. *et al.* The Link between NAFLD and Metabolic Syndrome. *Diagnostics* **13**, 614 (2023).

This article is protected by copyright. All rights reserved.

Accepted Manuscript

8. Ghazanfar, H. *et al.* Metabolic Dysfunction-Associated Steatohepatitis and Progression to Hepatocellular Carcinoma: A Literature Review. *Cancers* **16**, 1214 (2024).

9. Madir, A., Grgurevic, I., Tsochatzis, E. A. & Pinzani, M. Portal hypertension in patients with nonalcoholic fatty liver disease: Current knowledge and challenges. *World J. Gastroenterol.* **30**, 290–307 (2024).

10. Kleiner, D. E. *et al.* Design and validation of a histological scoring system for nonalcoholic fatty liver disease. *Hepatology* **41**, 1313–1321 (2005).

11. Bedossa, P. *et al.* Histopathological algorithm and scoring system for evaluation of liver lesions in morbidly obese patients. *Hepatology* **56**, 1751–1759 (2012).

12. Bravo, A. A., Sheth, S. G. & Chopra, S. Liver Biopsy. *New Engl J Medicine* **344**, 495–500 (2001).

13. Cusi, K. *et al.* American Association of Clinical Endocrinology Clinical Practice Guideline for the Diagnosis and Management of Nonalcoholic Fatty Liver Disease in Primary Care and Endocrinology Clinical Settings Co-Sponsored by the American Association for the Study of Liver Diseases (AASLD). *Endocr Pract* **28**, 528–562 (2022).

14. Ratziu, V. *et al.* Sampling Variability of Liver Biopsy in Nonalcoholic Fatty Liver Disease. *Gastroenterology* **128**, 1898–1906 (2005).

15. Merriman, R. B. *et al.* Correlation of paired liver biopsies in morbidly obese patients with suspected nonalcoholic fatty liver disease. *Hepatology* **44**, 874–880 (2006).

16. Larson, S. P. *et al.* Histopathologic Variability Between the Right and Left Lobes of the Liver in Morbidly Obese Patients Undergoing Roux-en-Y Bypass. *Clin Gastroenterol H* **5**, 1329–1332 (2007).

17. Grąt, K., Grąt, M. & Rowiński, O. Usefulness of Different Imaging Modalities in Evaluation of Patients with Non-Alcoholic Fatty Liver Disease. *Biomed* **8**, 298 (2020).

18. Imajo, K. *et al.* Magnetic Resonance Imaging More Accurately Classifies Steatosis and Fibrosis in Patients With Nonalcoholic Fatty Liver Disease Than Transient Elastography. *Gastroenterology* **150**, 626-637.e7 (2016).

19. Donnelly, K. L. *et al.* Sources of fatty acids stored in liver and secreted via lipoproteins in patients with nonalcoholic fatty liver disease. *J Clin Invest* **115**, 1343–1351 (2005).

20. Friedman, S. L., Neuschwander-Tetri, B. A., Rinella, M. & Sanyal, A. J. Mechanisms of NAFLD development and therapeutic strategies. *Nat Med* **24**, 908–922 (2018).

21. Sanyal, A. J. *et al.* Endpoints and clinical trial design for nonalcoholic steatohepatitis. *Hepatology* **54**, 344–353 (2011).

22. Yokoo, T. *et al.* Linearity, Bias, and Precision of Hepatic Proton Density Fat Fraction Measurements by Using MR Imaging: A Meta-Analysis. *Radiology* **286**, 486–498 (2017).

23. Park, C. C. *et al.* Magnetic Resonance Elastography vs Transient Elastography in Detection of Fibrosis and Noninvasive Measurement of Steatosis in Patients With Biopsy-Proven Nonalcoholic Fatty Liver Disease. *Gastroenterology* **152**, 598-607.e2 (2017).

This article is protected by copyright. All rights reserved.

Accepted Manuscript

24. Tang, A. *et al.* Nonalcoholic Fatty Liver Disease: MR Imaging of Liver Proton Density Fat Fraction to Assess Hepatic Steatosis. *Radiology* **267**, 422–431 (2013).

25. Martí-Aguado, D. *et al.* Automated Whole-Liver MRI Segmentation to Assess Steatosis and Iron Quantification in Chronic Liver Disease. *Radiology* **302**, 345–354 (2022).

26. McDonald, N. *et al.* Multiparametric magnetic resonance imaging for quantitation of liver disease: a two-centre cross-sectional observational study. *Sci Rep-uk* **8**, 9189 (2018).

27. Nogami, A. *et al.* Diagnostic comparison of vibration-controlled transient elastography and MRI techniques in overweight and obese patients with NAFLD. *Sci. Rep.* **12**, 21925 (2022).

28. Kim, B. K. *et al.* Clinical and histologic factors associated with discordance between steatosis grade derived from histology vs. MRI-PDFF in NAFLD. *Aliment. Pharmacol. Ther.* **58**, 229–237 (2023).

29. Noureddin, M. *et al.* Utility of magnetic resonance imaging versus histology for quantifying changes in liver fat in nonalcoholic fatty liver disease trials. *Hepatology* **58**, 1930–1940 (2013).

30. Fowler, K. J. *et al.* Repeatability of MRI Biomarkers in Nonalcoholic Fatty Liver Disease: The NIMBLE Consortium. *Radiology* **309**, e231092 (2023).

31. Hooker, J. C. *et al.* Inter-reader agreement of magnetic resonance imaging proton density fat fraction and its longitudinal change in a clinical trial of adults with nonalcoholic steatohepatitis. *Abdom Radiol* **44**, 482–492 (2019).

32. Pournik, O. *et al.* Inter-observer and Intra-observer Agreement in Pathological Evaluation of Non-alcoholic Fatty Liver Disease Suspected Liver Biopsies. *Hepat Mon* **14**, e15167 (2018).

33. Caussy, C., Reeder, S. B., Sirlin, C. B. & Loomba, R. Noninvasive, Quantitative Assessment of Liver Fat by MRI-PDFF as an Endpoint in NASH Trials. *Hepatology* **68**, 763–772 (2018).

34. Diefenbach, M. N., Liu, C. & Karampinos, D. C. Generalized parameter estimation in multi-echo gradient-echo-based chemical species separation. *Quantitative Imaging Medicine Surg* **10**, 554–567 (2020).

35. Leporq, B., Lambert, S. A., Ronot, M., Vilgrain, V. & Beers, B. E. V. Quantification of the triglyceride fatty acid composition with 3.0 T MRI. *Nmr Biomed.* **27**, 1211–1221 (2014).

36. Schneider, M. *et al.* Accurate fatty acid composition estimation of adipose tissue in the abdomen based on bipolar multi-echo MRI. *Magn. Reson. Med.* **81**, 2330–2346 (2019).

37. Fridén, M. *et al.* Hepatic Unsaturated Fatty Acids Are Linked to Lower Degree of Fibrosis in Non-alcoholic Fatty Liver Disease. *Frontiers Medicine* **8**, 814951 (2022).

38. Vilar-Gomez, E. *et al.* Fibrosis Severity as a Determinant of Cause-Specific Mortality in Patients With Advanced Nonalcoholic Fatty Liver Disease: A Multi-National Cohort Study. *Gastroenterology* **155**, 443-457.e17 (2018).

39. Marti-Aguado, D., Rodríguez-Ortega, A., Alberich-Bayarri, A. & Marti-Bonmati, L. Magnetic Resonance imaging analysis of liver fibrosis and inflammation: overwhelming gray zones restrict clinical use. *Abdom Radiol* **45**, 3557–3568 (2020).

This article is protected by copyright. All rights reserved.

Accepted Manuscript

40. Caldwell, S. *et al.* Hepatocellular ballooning in NASH. *J Hepatol* **53**, 719–723 (2010).

41. Alsaqal, S. *et al.* The Combination of MR Elastography and Proton Density Fat Fraction Improves Diagnosis of Nonalcoholic Steatohepatitis. *J Magn Reson Imaging* (2021) doi:10.1002/jmri.28040.

42. Loomba, R. *et al.* Multicenter Validation of Association Between Decline in MRI-PDFF and Histologic Response in NASH. *Hepatology* **72**, 1219–1229 (2020).

43. Dennis, A. *et al.* Correlations Between MRI Biomarkers PDFF and cT1 With Histopathological Features of Non-Alcoholic Steatohepatitis. *Front Endocrinol* **11**, 575843 (2021).

44. Jayakumar, S. *et al.* Longitudinal correlations between MRE, MRI-PDFF, and liver histology in patients with non-alcoholic steatohepatitis: Analysis of data from a phase II trial of selonsertib. *J Hepatol* **70**, 133–141 (2019).

45. Pepin, K. M., Welle, C. L., Guglielmo, F. F., Dillman, J. R. & Venkatesh, S. K. Magnetic resonance elastography of the liver: everything you need to know to get started. *Abdom Radiol* 1–21 (2021) doi:10.1007/s00261-021-03324-0.

46. Manduca, A. *et al.* MR elastography: Principles, guidelines, and terminology. *Magn. Reson. Med.* **85**, 2377–2390 (2021).

47. Allen, A. M. *et al.* The Role of Three-Dimensional Magnetic Resonance Elastography in the Diagnosis of Nonalcoholic Steatohepatitis in Obese Patients Undergoing Bariatric Surgery. *Hepatology* **71**, 510–521 (2020).

48. Yin, M. *et al.* Distinguishing between Hepatic Inflammation and Fibrosis with MR Elastography. *Radiology* **284**, 694–705 (2017).

49. Ichikawa, S. *et al.* Hepatitis activity should be considered a confounder of liver stiffness measured with MR elastography. *J. Magn. Reson. Imaging* **41**, 1203–1208 (2015).

50. Ulmenstein, S. von *et al.* Assessment of hepatic fibrosis and inflammation with look-locker T1 mapping and magnetic resonance elastography with histopathology as reference standard. *Abdom Radiol* **47**, 3746–3757 (2022).

51. Shi, Y. *et al.* Three-dimensional MR Elastography Depicts Liver Inflammation, Fibrosis, and Portal Hypertension in Chronic Hepatitis B or C. *Radiology* **301**, 154–162 (2021).

52. Alsaqal, S. *et al.* The Combination of MR Elastography and Proton Density Fat Fraction Improves Diagnosis of Nonalcoholic Steatohepatitis. *J Magn Reson Imaging* (2021) doi:10.1002/jmri.28040.

53. Dzyubak, B. *et al.* Automated Analysis of Multiparametric Magnetic Resonance Imaging/Magnetic Resonance Elastography Exams for Prediction of Nonalcoholic Steatohepatitis. *J Magn Reson Imaging* **54**, 122–131 (2021).

54. Breit, H. C. *et al.* Evaluation of liver fibrosis and cirrhosis on the basis of quantitative T1 mapping: Are acute inflammation, age and liver volume confounding factors? *Eur J Radiol* **141**, 109789 (2021).

55. Hoad, C. L. *et al.* A study of T1 relaxation time as a measure of liver fibrosis and the influence of confounding histological factors. *Nmr Biomed* **28**, 706–714 (2015).

This article is protected by copyright. All rights reserved.

Accepted Manuscript

56. Eddowes, P. J. *et al.* Utility and cost evaluation of multiparametric magnetic resonance imaging for the assessment of non-alcoholic fatty liver disease. *Aliment Pharm Therap* **47**, 631–644 (2018).

57. Wan, Q. *et al.* Water Specific MRI T1 Mapping for Evaluating Liver Inflammation Activity Grades in Rats With Methionine-Choline-Deficient Diet-Induced Nonalcoholic Fatty Liver Disease. *J. Magn. Reson. Imaging* **56**, 1429–1436 (2022).

58. Welle, C. L., Guglielmo, F. F. & Venkatesh, S. K. MRI of the liver: choosing the right contrast agent. *Abdom Radiol* **45**, 384–392 (2020).

59. Ulloa, J. L. *et al.* Assessment of gadoxetate DCE-MRI as a biomarker of hepatobiliary transporter inhibition. *Nmr Biomed.* **26**, 1258–1270 (2013).

60. Yamada, T. *et al.* Gd-EOB-DTPA-enhanced-MR imaging in the inflammation stage of nonalcoholic steatohepatitis (NASH) in mice. *Magn Reson Imaging* **34**, 724–729 (2016).

61. Ba-Ssalamah, A. *et al.* Hepatic gadoxetic acid uptake as a measure of diffuse liver disease: Where are we? *J. Magn. Reson. Imaging* **45**, 646–659 (2017).

62. Eming, S. A., Wynn, T. A. & Martin, P. Inflammation and metabolism in tissue repair and regeneration. *Science* **356**, 1026–1030 (2017).

63. Schuppan, D., Surabattula, R. & Wang, X. Y. Determinants of fibrosis progression and regression in NASH. *J Hepatol* **68**, 238–250 (2018).

64. Rohm, T. V., Meier, D. T., Olefsky, J. M. & Donath, M. Y. Inflammation in obesity, diabetes, and related disorders. *Immunity* **55**, 31–55 (2022).

65. Parthasarathy, G., Revelo, X. & Malhi, H. Pathogenesis of Nonalcoholic Steatohepatitis: An Overview. *Hepatology Commun* **4**, 478–492 (2020).

66. Schwabe, R. F., Tabas, I. & Pajvani, U. B. Mechanisms of Fibrosis Development in Nonalcoholic Steatohepatitis. *Gastroenterology* **158**, 1913–1928 (2020).

67. Marra, F. & Svegliati-Baroni, G. Lipotoxicity and the gut-liver axis in NASH pathogenesis. *J Hepatol* **68**, 280–295 (2018).

68. Minicis, S. *et al.* Dysbiosis contributes to fibrogenesis in the course of chronic liver injury in mice. *Hepatology* **59**, 1738–1749 (2014).

69. Lade, A., Noon, L. A. & Friedman, S. L. Contributions of metabolic dysregulation and inflammation to nonalcoholic steatohepatitis, hepatic fibrosis, and cancer. *Curr Opin Oncol* **26**, 100–107 (2014).

70. Hagström, H. *et al.* Fibrosis stage but not NASH predicts mortality and time to development of severe liver disease in biopsy-proven NAFLD. *J Hepatol* **67**, 1265–1273 (2017).

71. Parola, M. & Pinzani, M. Liver fibrosis: Pathophysiology, pathogenetic targets and clinical issues. *Mol Aspects Med* **65**, 37–55 (2019).

72. Imajo, K. *et al.* Direct Comparison of US and MR Elastography for Staging Liver Fibrosis in Patients With Nonalcoholic Fatty Liver Disease. *Clin Gastroenterol H* **20**, 908-917.e11 (2022).

This article is protected by copyright. All rights reserved.

Accepted Manuscript

73. Cui, J. *et al.* Magnetic resonance elastography is superior to acoustic radiation force impulse for the Diagnosis of fibrosis in patients with biopsy-proven nonalcoholic fatty liver disease: A prospective study. *Hepatology* **63**, 453–461 (2016).

74. Loomba, R. *et al.* Magnetic resonance elastography predicts advanced fibrosis in patients with nonalcoholic fatty liver disease: A prospective study. *Hepatology* **60**, 1920–1928 (2014).

75. Costa-Silva, L., Ferolla, S. M., Lima, A. S., Vidigal, P. V. T. & Ferrari, T. C. de A. MR elastography is effective for the non-invasive evaluation of fibrosis and necroinflammatory activity in patients with nonalcoholic fatty liver disease. *Eur J Radiol* **98**, 82–89 (2018).

76. Loomba, R. *et al.* Novel 3D Magnetic Resonance Elastography for the Noninvasive Diagnosis of Advanced Fibrosis in NAFLD: A Prospective Study. *Am J Gastroenterol* **111**, 986–994 (2016).

77. Hoffman, D. H. *et al.* T1 mapping, T2 mapping and MR elastography of the liver for detection and staging of liver fibrosis. *Abdom Radiol* **45**, 692–700 (2020).

78. Huwart, L. *et al.* Magnetic Resonance Elastography for the Noninvasive Staging of Liver Fibrosis. *Gastroenterology* **135**, 32–40 (2008).

79. Venkatesh, S. K., Yin, M. & Ehman, R. L. Magnetic resonance elastography of liver: Technique, analysis, and clinical applications. *J. Magn. Reson. Imaging* **37**, 544–555 (2013).

80. Taylor, A. J., Salerno, M., Dharmakumar, R. & Jerosch-Herold, M. T1 Mapping Basic Techniques and Clinical Applications. *Jacc Cardiovasc Imaging* **9**, 67–81 (2016).

81. Banerjee, R. *et al.* Multiparametric magnetic resonance for the non-invasive diagnosis of liver disease. *J Hepatol* **60**, 69–77 (2014).

82. Mózes, F. E. & Tunnicliffe, E. M. Differences between T1 and corrected T1 cannot be attributed to iron-correction only. *Pediatr Radiol* **51**, 499–500 (2021).

83. Dennis, A. *et al.* Correlations Between MRI Biomarkers PDFF and cT1 With Histopathological Features of Non-Alcoholic Steatohepatitis. *Front Endocrinol* **11**, 575843 (2021).

84. Pavlides, M. *et al.* Multiparametric magnetic resonance imaging for the assessment of non-alcoholic fatty liver disease severity. *Liver Int* **37**, 1065–1073 (2017).

85. Perspectum. LiverMultiScan v5.0 - Interpreting Liver Tissue Characterization for Physicians. Preprint at (2023).

86. Beer, L. *et al.* Inter- and intra-reader agreement for gadoxetic acid–enhanced MRI parameter readings in patients with chronic liver diseases. *Eur. Radiol.* **29**, 6600–6610 (2019).

87. Verloh, N. *et al.* Liver fibrosis and Gd-EOB-DTPA-enhanced MRI: A histopathologic correlation. *Sci Rep-uk* **5**, 15408 (2015).

88. Ringe, K. I., Husarik, D. B., Gupta, R. T., Boll, D. T. & Merkle, E. M. Hepatobiliary transit times of gadoxetate disodium (Primovist®) for protocol optimization of comprehensive MR imaging of the biliary system—What is normal? *Eur J Radiol* **79**, 201–205 (2011).

This article is protected by copyright. All rights reserved.

Accepted Manuscript

89. Tsuda, N., Okada, M. & Murakami, T. New proposal for the staging of nonalcoholic steatohepatitis: Evaluation of liver fibrosis on Gd-EOB-DTPA-enhanced MRI. *Eur J Radiol* **73**, 137–142 (2010).

90. Tsuda, N. & Matsui, O. Signal profile on Gd-EOB-DTPA-enhanced MR imaging in non-alcoholic steatohepatitis and liver cirrhosis induced in rats: correlation with transporter expression. *Eur. Radiol.* **21**, 2542–2550 (2011).

91. Chen, B.-B. *et al.* Dynamic contrast-enhanced magnetic resonance imaging with Gd-EOB-DTPA for the evaluation of liver fibrosis in chronic hepatitis patients. *Eur. Radiol.* **22**, 171–180 (2012).

92. Koh, D.-M. *et al.* Consensus report from the 9th International Forum for Liver Magnetic Resonance Imaging: applications of gadoxetic acid-enhanced imaging. *Eur Radiol* 1–14 (2021) doi:10.1007/s00330-020-07637-4.

93. Schneider, C. V. *et al.* Prevalence of at-risk MASH, MetALD and alcohol-associated steatotic liver disease in the general population. *Aliment. Pharmacol. Ther.* (2024) doi:10.1111/apt.17958.

94. Loomba, R. *et al.* Safety, pharmacokinetics, and pharmacodynamics of pegozafermin in patients with non-alcoholic steatohepatitis: a randomised, double-blind, placebo-controlled, phase 1b/2a multiple-ascending-dose study. *Lancet Gastroenterol. Hepatol.* **8**, 120–132 (2023).

95. Nedrud, M. A. *et al.* MRI Quantification of Placebo Effect in Nonalcoholic Steatohepatitis Clinical Trials. *Radiology* 220743 (2022) doi:10.1148/radiol.220743.

96. Stine, J. G. *et al.* Change in MRI-PDFF and Histologic Response in Patients with Nonalcoholic Steatohepatitis: A Systematic Review and Meta-Analysis. *Clin Gastroenterol H* **19**, 2274-2283.e5 (2020).

97. Lee, S. W. *et al.* Low liver fat in non-alcoholic steatohepatitis-related significant fibrosis and cirrhosis is associated with hepatocellular carcinoma, decompensation and mortality. *Aliment. Pharmacol. Ther.* **59**, 80–88 (2024).

98. Ajmera, V. *et al.* Liver Stiffness on Magnetic Resonance Elastography and the MEFIB Index and Liver-Related Outcomes in Nonalcoholic Fatty Liver Disease: A Systematic Review and Meta-Analysis of Individual Participants. *Gastroenterology* **163**, 1079-1089.e5 (2022).

99. Ajmera, V. *et al.* Prognostic utility of magnetic resonance elastography and MEFIB index in predicting liver-related outcomes and mortality in individuals at risk of and with nonalcoholic fatty liver disease. *Ther. Adv. Gastroenterol.* **15**, 17562848221093868 (2022).

100. Kim, B. K. *et al.* Magnetic resonance elastography-based prediction model for hepatic decompensation in NAFLD: A multicenter cohort study. *Hepatology* **78**, 1858–1866 (2023).

101. Nogami, A. *et al.* Noninvasive imaging biomarkers for liver steatosis in NAFLD: present and future. *Clin Mol Hepatology* (2022) doi:10.3350/cmh.2022.0357.

102. 2_National_schedule_of_NHS_costs_FY21-22_v3.xlsx. https://view.officeapps.live.com/op/view.aspx?src=https%3A%2F%2Fwww.england.nhs.uk%2Fwp-content%2Fuploads%2F2023%2F04%2F2_National_schedule_of_NHS_costs_FY21-22_v3.xlsx&wdOrigin=BROWSELINK.

This article is protected by copyright. All rights reserved.

Accepted Manuscript

103. Vilar-Gomez, E. *et al.* Cost Effectiveness of Different Strategies for Detecting Cirrhosis in Patients With Nonalcoholic Fatty Liver Disease Based on United States Health Care System. *Clin Gastroenterol H* **18**, 2305-2314.e12 (2020).

104. Loomba, R. *et al.* MASH Resolution Index: development and validation of a non-invasive score to detect histological resolution of MASH. *Gut* gutjnl-2023-331401 (2024) doi:10.1136/gutjnl-2023-331401.

105. Huang, D. Q. *et al.* Clinical Utility of Combined MRI-PDFF and ALT Response in Predicting Histologic Response in Nonalcoholic Fatty Liver Disease. *Clin. Gastroenterol. Hepatol.* **21**, 2682-2685.e4 (2023).

106. Noureddin, M. *et al.* MRI-based (MAST) score accurately identifies patients with NASH and significant fibrosis. *J Hepatol* (2021) doi:10.1016/j.jhep.2021.11.012.

107. Tamaki, N. *et al.* Magnetic resonance elastography plus Fibrosis-4 versus FibroScan–aspartate aminotransferase in detection of candidates for pharmacological treatment of NASH-related fibrosis. *Hepatology* **75**, 661–672 (2022).

108. Noureddin, N. *et al.* MEFIB-Index and MAST-Score in the assessment of hepatic decompensation in metabolic dysfunction-associated steatosis liver disease—Individual participant data meta-analyses. *Aliment. Pharmacol. Ther.* **58**, 856–865 (2023).

109. Brand, T. *et al.* Superficial vs Deep Subcutaneous Adipose Tissue: Sex-Specific Associations With Hepatic Steatosis and Metabolic Traits. *J Clin Endocrinol Metabolism* **106**, e3881–e3889 (2021).

110. Idilman, I. S. *et al.* Association between Visceral Adipose Tissue and Non-Alcoholic Steatohepatitis Histology in Patients with Known or Suspected Non-Alcoholic Fatty Liver Disease. *J Clin Medicine* **10**, 2565 (2021).

111. Tordjman, J., Guerre-Millo, M. & Clément, K. Adipose tissue inflammation and liver pathology in human obesity. *Diabetes Metab* **34**, 658–663 (2008).

112. Mauro, E. & Gadano, A. What's new in portal hypertension? *Liver Int* **40**, 122–127 (2020).

113. Ronot, M. *et al.* Assessment of portal hypertension and high-risk oesophageal varices with liver and spleen three-dimensional multifrequency MR elastography in liver cirrhosis. *Eur. Radiol.* **24**, 1394–1402 (2014).

Figure 1. Forest plots of pooled diagnostic sensitivity and specificity for the prediction of different steatosis stages using MRI-PDFF. Data was processed using Met DiSc 2.0. MRI, magnetic resonance imaging; PDFF, proton density fat fraction.

Figure 2. Forest plots of pooled diagnostic sensitivity and specificity for the prediction of different fibrosis stages using MRE. Data was processed using Met DiSc 2.0. MRE, magnetic resonance elastography.

This article is protected by copyright. All rights reserved.
Accepted Manuscript

Figure 3. Schematic illustration of the applicability of different MRI modalities (PDFF, (c)T_1 and MRE) throughout the MASLD spectrum. The figure shows that while there is overlap between the applicability of each modality, each has its own strengths and weaknesses depending on the stage of the disease. cT_1, iron-corrected T_1; MASH, metabolic dysfunction associated steatohepatitis; MASLD, metabolic dysfunction associated steatotic liver disease; MRE, magnetic resonance elastography; MRI, magnetic resonance imaging; PDFF, proton density fat fraction; T_1, longitudinal relaxation time.

Figure 4. Illustration of how a multiparametric MRI protocol covering tissue composition (i.e., fat content and extracellular water), tissue mechanical properties and hepatocyte function evaluation of the liver (outer ring) can cover the features accessed by histology (center: steatosis, activity and fibrosis). Thereby adding an additional measure by the assessment of hepatocyte function. MRI, magnetic resonance imaging.

Figure 5. Net plots providing an overview of the performance of the determination of different features of MASLD (A) and methodological criteria (B) comparing the MRI techniques (PDFF, (c)T_1, MRE and Gadoxetate) to liver biopsy. Inspired by Nogami et al.[101]. cT_1, iron-corrected T_1; MASLD, metabolic dysfunction associated steatotic liver disease; MRE, magnetic resonance elastography; MRI, magnetic resonance imaging; PDFF, proton density fat fraction; T_1, longitudinal relaxation time.

Table 1. MRI methods for evaluation of MASLD

	MRI-PDFF	MRE	Gadoxetate	(c)T_1
Description	Relative measure of MR signal originating from triglycerides	Supplemental device that allows the measurement of tissue mechanical properties	Contrast agent that is actively taken up by healthy hepatocytes	MR signal property sensitive to changes in extracellular water
Measurements	Fat fraction (fat/(fat & water))	Tissue mechanical	Hepatocyte	Extracellular

This article is protected by copyright. All rights reserved.

Accepted Manuscript

		properties	function	water
Assessed MASLD feature(s)	Steatosis, Ballooning	Fibrosis, Inflammation	Fibrosis, Inflammation, Hepatocyte Function	Fibrosis, Inflammation
Strengths	Full organ coverage, accepted/validated biomarker for liver steatosis	Full organ coverage, diagnostic accuracy	Full organ coverage, measure of liver function	Full organ coverage
Challenges	Additional vendor packages required (cost & availability)	Additional hardware required (cost & availability), Confounded by • Edema • Iron (mainly at 3T)	Contrast injection, exploratory, complex, advanced mathematical model required for dynamic imaging	Confounded by • Fat load • Iron (only T_1) • Hydration • Glycogen • Edema cT_1: patented commercial product (cost & availability)
Opportunities	Differentiation of abdominal adipose tissue compartments &	Combination with circulating biomarkers, Extraction of	Assessment of liver function, Multiple physiological	Bridging the gap between PDFF & MRE, Assessment of

This article is protected by copyright. All rights reserved.

Accepted Manuscript

	fatty acid composition	different measures, 3D MRE, Indication for portal hypertension derivable when extending MRE to the spleen	parameters accessible with compartmental analysis, Simultaneous screening for hepatocellular carcinomas	inflammatory status of (visceral) adipose tissue

cT_1, iron-corrected T_1; MASLD, metabolic dysfunction associated steatotic liver disease; MRE, magnetic resonance elastography; MRI, magnetic resonance imaging; PDFF, proton density fat fraction; T_1, longitudinal relaxation time.

This article is protected by copyright. All rights reserved.

Accepted Manuscript

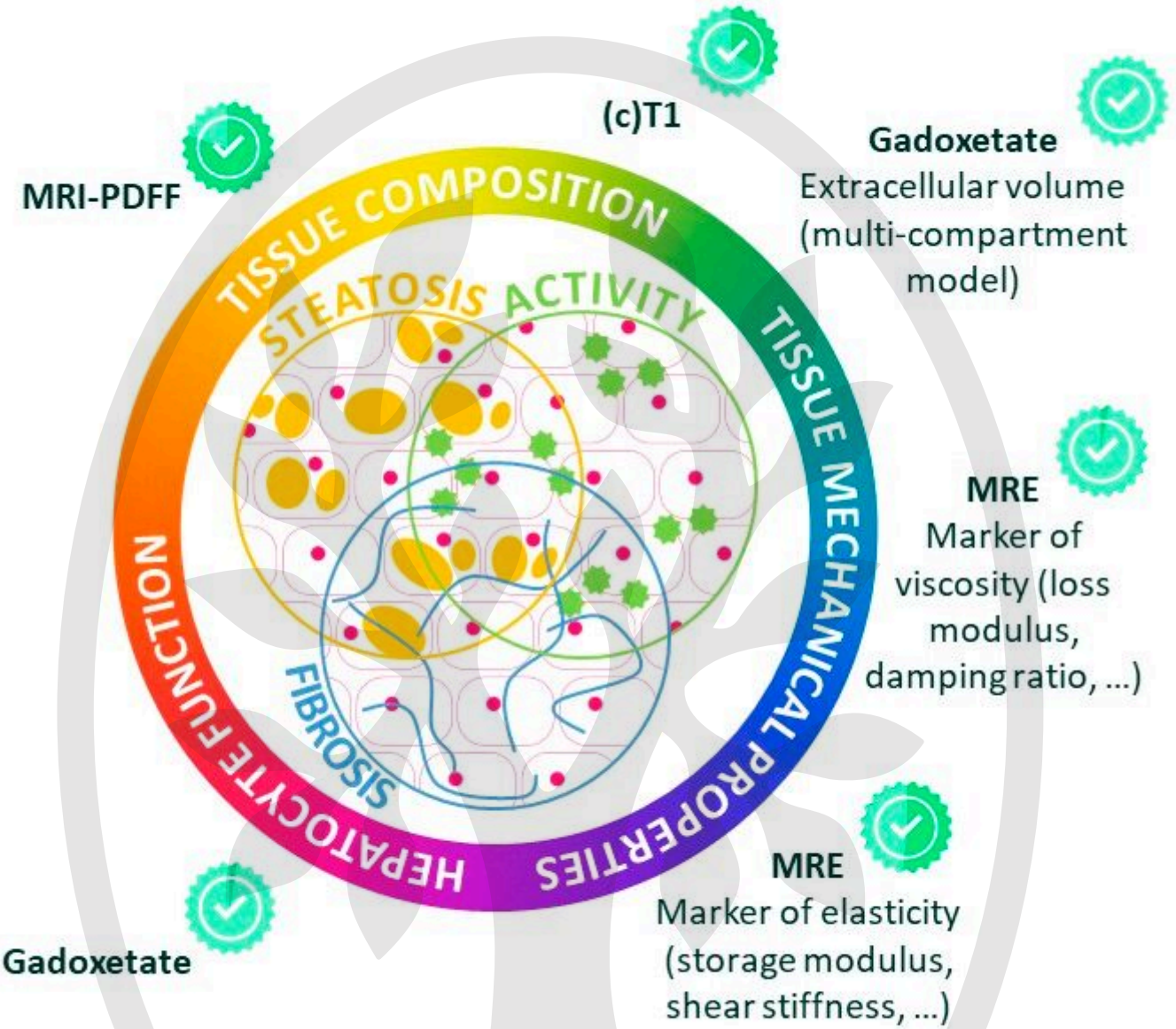

This article is protected by copyright. All rights reserved.

Accepted Manuscript